THE JOURNAL OF PHYSICAL CHEMISTRY Letters

Letter

Deciphering Front-Side Complex Formation in S2 Reactions via Dynamics Mapping

Istvan Szabo, Balazs Olasz, and Gabor Czako

J. Phys. Chem. Lett., **Just Accepted Manuscript** • Publication Date (Web): 09 Jun 2017

ACS Publications

The Journal of Physical Chemistry Letters is published by the American Chemical Society. 1155 Sixteenth Street N.W., Washington, DC 20036

Deciphering Front-Side Complex Formation in S_N2 Reactions via Dynamics Mapping

*István Szabó**,†, Balázs Olasz‡ and Gábor Czakó**‡

†Department of Chemistry, King's College London, London SE1 1DB, UK

‡Department of Physical Chemistry and Materials Science, Institute of Chemistry, University of Szeged, Rerrich Béla tér 1, Szeged H-6720, Hungary

ABSTRACT

Due to their importance in organic chemistry the atomistic understanding of bimolecular nucleophilic substitution (S_N2) reactions shows exponentially growing interest. In this publication the effect of front-side complex (FSC) formation is uncovered via quasi-classical trajectory computations combined with a novel analysis method called trajectory orthogonal projection (TOP). For both F^- + CH_3Y [Y=Cl,I] reactions the life time distributions of the F^---YCH_3 front-side complex revealed weakly trapped nucleophiles (F^-). However, only the F^- + CH_3I reaction features strongly trapped nucleophiles in the front-side region of the prereaction well. Interestingly, both back-side and front-side attack show propensity to long-lived FSC formation. Spatial distributions of the nucleophile demonstrate more prominent FSC formation in case of the F^- + CH_3I reaction compared to F^- + CH_3Cl. The presence of front-side intermediates and the broad spatial distribution in the back-side region may explain the indirect nature of the F^- + CH_3I reaction.

TOC GRAPHICS

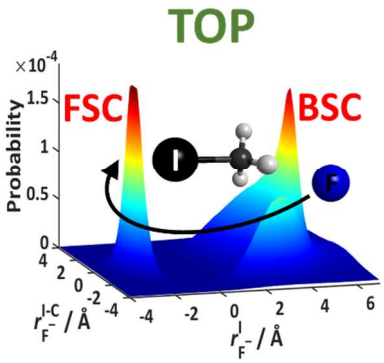

KEYWORDS mechanism, nucleophilic substitution, ion-dipole complex, front-side intermediate, quasi-classical, trajectory projection, life time, Nu^- capture

Ion-dipole bimolecular nucleophilic substitution (S_N2) is among the most prevalent reaction pathways in chemistry and biochemistry.[1-6] However, unlike what is suggested in organic chemistry textbooks the dynamics of these reactions are quite complex.[7-10] A general overall S_N2 reaction can be written as $Nu^- + CH_3Y \rightarrow CH_3Nu + Y^-$, where Nu^- and Y denote the attacking nucleophile and the leaving group, respectively. Potential energy landscape for this family of reactions is comprised of a central barrier which separates the pre- and postreaction wells. According to our current atomistic understanding, reactive events usually begin with the attack of the Nu^- nucleophile on the methyl side of CH_3Y forming ion-dipole (Nu^---H_3CY) and/or hydrogen-bonded (Nu^---HCH_2Y) pre-reaction complexes then the system goes through the central transition state $[Nu\text{--}CH_3\text{--}Y]^-$, where synchronously a new Nu-C bond forms and the C-Y bond breaks, while the umbrella motion around the sp^3 carbon center inverts the configuration. At higher translational energies the endothermic H-abstraction and the front-side attack channels open. The later pathway leads to retention of the final configuration, as well as the double-inversion mechanism revealed by our dynamics simulations[8] in gas phase and recently confirmed also in aqueous solution.[11]

Recently, the F^- + CH_3Cl and F^- + CH_3I S_N2 reactions were probed with combined crossed-beam imaging and molecular dynamics simulations providing interesting clues to the overall dynamics of S_N2 reactions at an atomistic level.[9] Both reactions are highly exothermic and characterized by a similar potential energy landscape with a C_s-symmetric H-bonded complex in the entrance channel together with the traditional close-lying ion-dipole complex of C_{3v} symmetry connected by a low-barrier transition state. Despite of these similarities, the dynamics of the two reactions showed substantial differences, which indicated the influence of the leaving group in the S_N2 mechanism even in the entrance channel. In case of the F^- + CH_3Cl S_N2

reaction we have found that at low collision energies the indirect mechanism dominates, whereas at higher collision energies the reaction mainly occurs via the direct rebound mechanism.[9,12] In contrast, for the F^- + CH_3I S_N2 reaction a major contribution of the indirect mechanism to the total cross-section was observed at all collision energies investigated supported by the product velocity, scattering angle and product internal energy distributions.[9,12,13] These unexpected qualitative differences were putatively explained based on the differences in dipole moments which might affect the orientation of the reactants. However, the observed changes in mechanism were not completely clarified.[9] Very recently, Xie and Hase envisioned in their perspective article[10] the determining role of the front-side complexes to suppress back-side attack and the roundabout mechanism accordingly. Front-side complexes have been recognized for assisting in dihalide formation in the F^- + CF_3Br, F^- + CF_3I, and Cl^- + CF_3Br reactions.[14-16] Detailed unimolecular dynamics with lifetime distributions were determined for the $[CH_3$--I--$OH]^-$ front-side complex by Hase and co-workers.[17] Moreover, FSCs were proposed to explain the indirect nature of several prototypical S_N2 reactions, *e.g.* OH^- + CH_3I,[17-19] and F^- + CH_3I,[13] but the exact causes of the observed differences in the mechanism remained unclear. Our aim is to provide a detailed characterization of the structure and energetics of the Nu^---YCH_3 [Nu=F,Cl,Br,I; Y=Cl,Br,I] front-side complex minima and to explore the fascinating mechanistic roles of these intermediate ion-dipole complexes on the example of the prototypical F^---YCH_3 [Y=Cl,I] S_N2 reactions. Of particular interest is the time-scale of the trapping in the front-side pre-reaction well.

Potential energy surfaces of the Nu^- + CH_3Y [Nu=F,Cl,Br,I; Y=Cl,Br,I] reactions feature a potential energy well in the front-side region, *i.e.* in close proximity of the leaving group. Relative energies of the corresponding minima strongly depend on the nucleophile and also the

leaving group. As shown in Figure 1a, the F^- + CH_3I reaction has a front-side complex with a potential energy minimum of −22.8 kcal mol^{-1}, relative to the reactants, and the equivalent FSC minimum for the F^- + CH_3Cl reaction is only −2.7 kcal mol^{-1}, whereas the corresponding values on our chemically accurate analytical potential energy surfaces (PESs) are −22.6 and −3.7 kcal mol^{-1}, respectively.[13] Considering all the possible Nu^---YCH_3 [Nu=F,Cl,Br,I; Y=Cl,Br,I] front-side minima (shown in Figure S1) the $[F\text{--}ICH_3]^-$ has the deepest minimum, followed by the F^---$BrCH_3$ and Cl^---ICH_3 complexes characterized by a potential energy minimum of −10.7 and −9.2 kcal mol^{-1}, respectively. Note that the aforementioned OH^---ICH_3 long-lived intermediate complex is characterized by an even deeper potential minimum of −26.1 kcal mol^{-1}, predicted by DFT based methods.[17] (The corresponding value is −24.1 kcal mol^{-1} at the CCSD(T)-F12b/aug-cc-pVTZ(-PP) level of theory.) Regarding the structure of F^---YCH_3 [Y=Cl,I], the F-I bond length is 0.191 Å longer than the F-Cl distance. The Cl-C/I-C bond length in F^---YCH_3 [Y=Cl,I] is 0.006/0.077 Å shorter than the corresponding bond in CH_3Cl/CH_3I. According to the Natural Bond Orbital population analysis of F^---YCH_3 [Y=Cl,I] the Cl and I atoms carry a partial charge of +0.02 and +0.25, respectively, whereas the H atoms carry +0.16 for both front-side intermediates. In contrast to the F^---ICH_3 ion-dipole complex, the negative charge is distributed disproportionately between the F and C atoms of the F^---$ClCH_3$ complex with −0.97 and −0.52, respectively.

To get insight into the energetics of the front-side attachment of the F^- ion to the methyl-halide in the entrance channel, the two-dimensional (2D) interaction potential was calculated by performing a scan of the PES with YCH_3 [Y=Cl,I] fixed in its equilibrium geometry. From the 2D interaction potentials depicted in Fig. 1c-f we can distinguish two deep wells for both reactions, corresponding to the interactions of the Nu^- nucleophile with the –CH_3 group and the

halogens (Y=Cl,I). It is clearly seen, that the back and front-side complex wells are separated by a potential-ridge, which intersects the halogen at both limiting F-C-Y-H dihedral angles (see Fig. 1b). On the $-CH_3$ side, the bottom of the potential energy well features the collinear ion-dipole and H-bonded pre-reaction complexes, which strongly influence the migration of the Nu^- between the BSC and FSC regions of the F^---YCH_3 [Y=Cl,I] S_N2 reactions.[9] In the front-side region the interaction potentials substantially deviate, due to the differences in the attraction of the two halogens. The nature of the complexation in this well is less well understood. Based on the shape of the interaction potential we hypothesised that the potential well in the front-side region is suitable to capture the approaching nucleophile in close proximity of the leaving group.

As we know, the trajectories may avoid even the deep potential minimum,[20] thus we cannot rely solely on the potential energy landscapes. Therefore, we are proposing an alternative approach, called trajectory orthogonal projection (TOP) to visualize and to quantify the nucleophilic attack in S_N2 reactions. Our methodology consists of the following simple steps: (1) quasi-classical trajectories are run at a given collision energy covering the impact parameter (b) range from 0 to the maximum value of b, where reactive event is likely to occur, (2) the three-dimensional positions of the nucleophile in the entrance channel are orthogonally projected to one- or two-dimensional subspaces defined by certain atoms of CH_3Y, (3) the distribution of the resulting positions is obtained by the standard Histogram Binning technique.[21] In fact, the TOP method aligns the reactive system to subspaces defined with the nuclei in the CH_3Y polyatomic reactant providing the spatial probability of nucleophilic attack around CH_3Y in a given point of the subspace. Spatial distributions in the subspaces like the line through the {Y,C} nuclei, the {Y,C,H} plane or the plane perpendicular to {Y,C,H} are all very informative in terms of mapping the effective dynamics of the system. One should emphasize that TOP is capable to

reveal reaction channels which are unlikely to follow the minimum energy path predicted by the potential energy landscape.

With analytical potential energy functions at hand for both F^- + CH_3Y [Y=Cl,I] reactions[8,13] we have a unique starting point to obtain statistically accurate spatial probability distributions. To shed light on the effective dynamics of these reactions, the trajectory orthogonal projection (TOP) method has been applied to the entrance channel of all the reactive S_N2 trajectories by imposing the following constraints on the internal coordinates of CH_3Y: $r_{C\text{-}I} < 3.5$ Å, and $\max(r_{C\text{-}H}) < 2.5$ Å in order to avoid the interference with the S_N2 exit-channel and the proton-abstraction pathway. (Note that the barrier of halogen abstraction is usually much higher than the maximum collision energy in this study.) In Fig. 2 the normalized spatial probability of the attacking Nu^- around CH_3Y (Y=Cl,I) is shown at collision energy of 1 kcal mol^{-1}. On the one hand, the distributions corresponding to the two reactions bear similarities in the back-side region, where both reactions show a characteristic peak which centers (red spot) on the C_3 axis of CH_3Y [Y=Cl,I] at a Nu^--I distance equal to the sum of $r_{I\text{-}C,eq}$ and $r_{C\text{-}Nu,eq}$ distances in the IH_3C--Nu^- prereaction ion-dipole complex. As also expected, a higher probability region emerges on the 2D map in close proximity of the H atom as an indicator of the extensive YH_2CH--Nu^- H-bonded complex formation. It is noteworthy that the Nu^- probability distribution in the BSC region is broader in case of the F^- + CH_3I reaction, which is consistent with the larger b_{max} values for this S_N2 reaction.[12,13] This increased chance for energy redistribution between the inter- and intramolecular modes of the pre-reaction complex may be a principal recipient of the more pronounced indirect nature of the F^- + CH_3I S_N2 reaction. On the other hand, in the front-side region the difference in Nu^- spatial distributions is striking. The F^- + CH_3I reaction features a prominent peak corresponding to the position of F^- in the F^---ICH_3 front-side ion-dipole

complex; however, in case of the F^- + CH_3Cl reaction the spatial distribution of F^- is completely isotropic in the front-side region. These findings are in line with the characteristics of the interaction potentials. The probability distributions for both reactions are qualitatively the same up to a collision energy of 15.9 kcal mol^{-1} (see Fig. S3-5). At higher collision energies (Fig. S6) the reaction is mainly direct suppressing the orientation effects, thus only those reactants lead to products, which start with back-side attack. Moreover, the dominant direct roundabout mechanism hinders the formation of ion-dipole and H-bonded complexes, and results in backward scattered products.[12,13]

An approach for investigating the time-scale of nucleophile capture is to consider the fraction of the trajectory spent in the FSC region.[22] Considering the shape of the interaction potential, as well as the spatial distribution of the nucleophile, the life time of the individual capture events is calculated from the trajectory integration times in the $r_{\mathrm{Nu}^-}^{\mathrm{Y}} < 0$ region, where $r_{\mathrm{Nu}^-}^{\mathrm{Y}}$ is the distance of the trapped Nu^- from the Y halogen atom after orthogonal projection to the {Y,C} line. We should emphasize, that our definition for the front-side region is not limited to the close proximity of the Y halogen atom, because after inspection of many trajectories we had to realize that the trapped trajectories span a long-range region of the configurational space. Nevertheless, the exact separation of the temporarily and strongly trapped trajectory segments is not straightforward. Although, this difficulty may eventually be overcome by analysing the residence time of the F^- ion in the FSC region. As seen on Fig. 3a and 3b, the life time distribution of individual front-side complexation events features two regions. Up to 4 and 2 ps for F^---ICH_3 and F^---$ClCH_3$, respectively, the short-lived transient complexes are represented by high probability peaks, but the probability instead of dropping to zero it extends to very large life times, denoted with $t_{\mathrm{FSC,max}}$, especially in case of the F^- + CH_3I reaction. These long-lived,

strongly trapped complexes have an isotropic life time distribution up to $t_{FSC,max}$ (not shown on the graphs) and show little E_{coll} dependence at moderate reactant translational energies. To track the differences in life time distributions for the two systems we performed QCT simulations with Cl of mass 127 a.u. (corresponding to I) using the $F^- + CH_3Cl$ PES.[23] As predicted before,[9] the mass-scaling has only minor effects on the life time distribution and $t_{FSC,max}$, thereby underpinning the role of the interaction potential. Considering the partitioning of the total life between short-lived and long-lived FSCs the two reactions differ dramatically. Interestingly, the strongly trapped $F^- + CH_3I$ trajectories constitute only about 1% of the FSC events; but it is truly impressive that they accumulate ~35% of the total FSC life time at a collision energy of 1.0 kcal mol^{-1} and ~55% at 15.9 kcal mol^{-1} considering the back-side and front-side attack trajectories together. Since the reaction becomes more direct at higher collision energies the fractions of life time corresponding to BSA trajectories are also increased. In case of the $F^- + CH_3Cl$ reaction the fraction of long-lived trajectories is almost negligible and the E_{coll} dependence of the life time fractions shows similar trend to the $F^- + CH_3I$ system.

Representative trajectories presented in Fig. 4 hold evidence for formation of the front-side intermediate complex on the example of the $F^- + CH_3I$ reaction at E_{coll} = 2 kcal mol^{-1}. As seen on panel a, even trajectories starting with back-side attack (red arrow) can easily get around the polyatomic reactant, CH_3I and after spending a short time in the front-side well can lead to reactive event. Another typical trajectory is shown on panels b and c projected to the {I,C,H(red)} plane and to the plane perpendicular to {I,C,H(red)}, respectively. Here, the F^- nucleophile approaches CH_3I from the halogen side and it is immediately captured in the front-side well for 42.1 ps. Note that this residence time is approximately 20 times larger than the trajectory integration time of a complete rebound or stripping process and it is comparable with

the time-scale of the indirect mechanism.[8,12,13] After dissociation of the F^---ICH_3 intermediate complex, the F^- ion leaves the front-side region being trapped for a short time in the back-side region of the pre-reaction well. Once its relative orientation to the permanent dipole becomes appropriate, the substitution event can take place by simultaneous C-F bond formation and C-I bond rupture.

Although, front-side intermediates assume a non-reactive ion-dipole orientation, the dynamics of S_N2 reactions at low collision energies is partially controlled by the nucleophile capture in the front-side region of the pre-reaction well. At the high collision energy regime (> 35 kcal mol^{-1}) the probability to find front-side complexes is lower, because the FSC formation is suppressed leading to shorter life times. We can conclude that FSC formation is a principal component of the indirect mechanism. It will be of great interest to investigate the effect of mode-specific excitation on the migration of the Nu^- in the pre-reaction well and quantum dynamics studies are also highly desired to analyse the resonant states in the front-side region.[24] In a wider context, the present proof of principle application of the trajectory orthogonal projection (TOP) method is a solid starting point to reveal reaction pathways and thoroughly understand the effective dynamics of the fundamentally important S_N2 reactions using dynamics mapping.

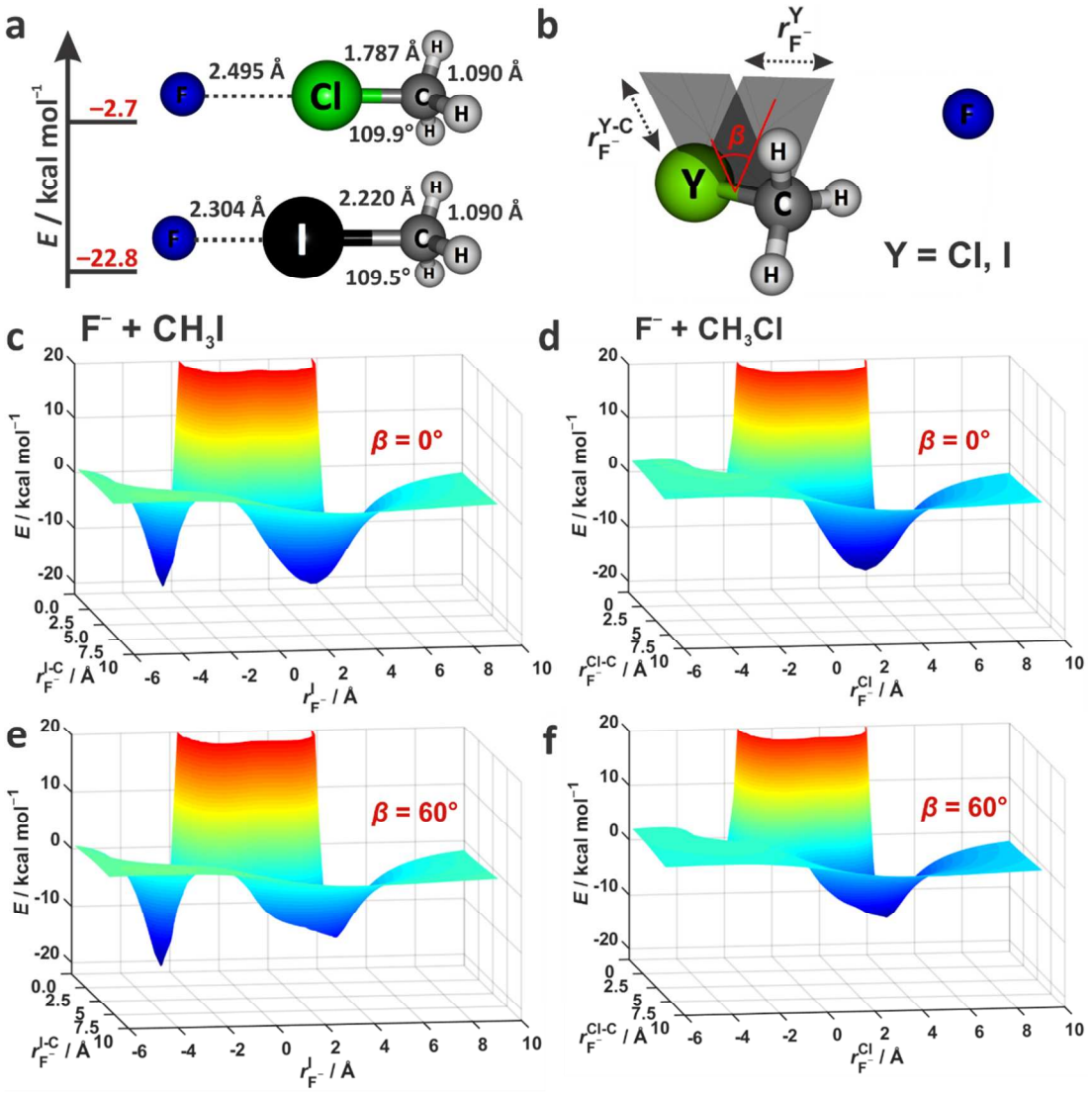

Figure 1. Structure and energetics of front-side complex (FSC) minima. (a) Structural parameters and energies relative to the F^- + CH_3Y(eq) [Y=Cl,I] reactant asymptote obtained at the CCSD(T)-F12b/aug-cc-pVTZ(-PP) level of theory (b-f) Entrance channel interaction potential energy scans of F^- + CH_3Y(eq) [Y=Cl,I] performed at the CCSD(T)-F12b/aug-cc-pVDZ(-PP) level of theory; the energies are relative to the F^- + CH_3Y(eq) reactant asymptote. (b) Definition of the potential energy surface scan. The structural parameters and relative energies of Nu^- + CH_3Y [Nu=F,Cl,Br,I; Y=Cl,Br,I] FSC minima are given in the Supporting Information.

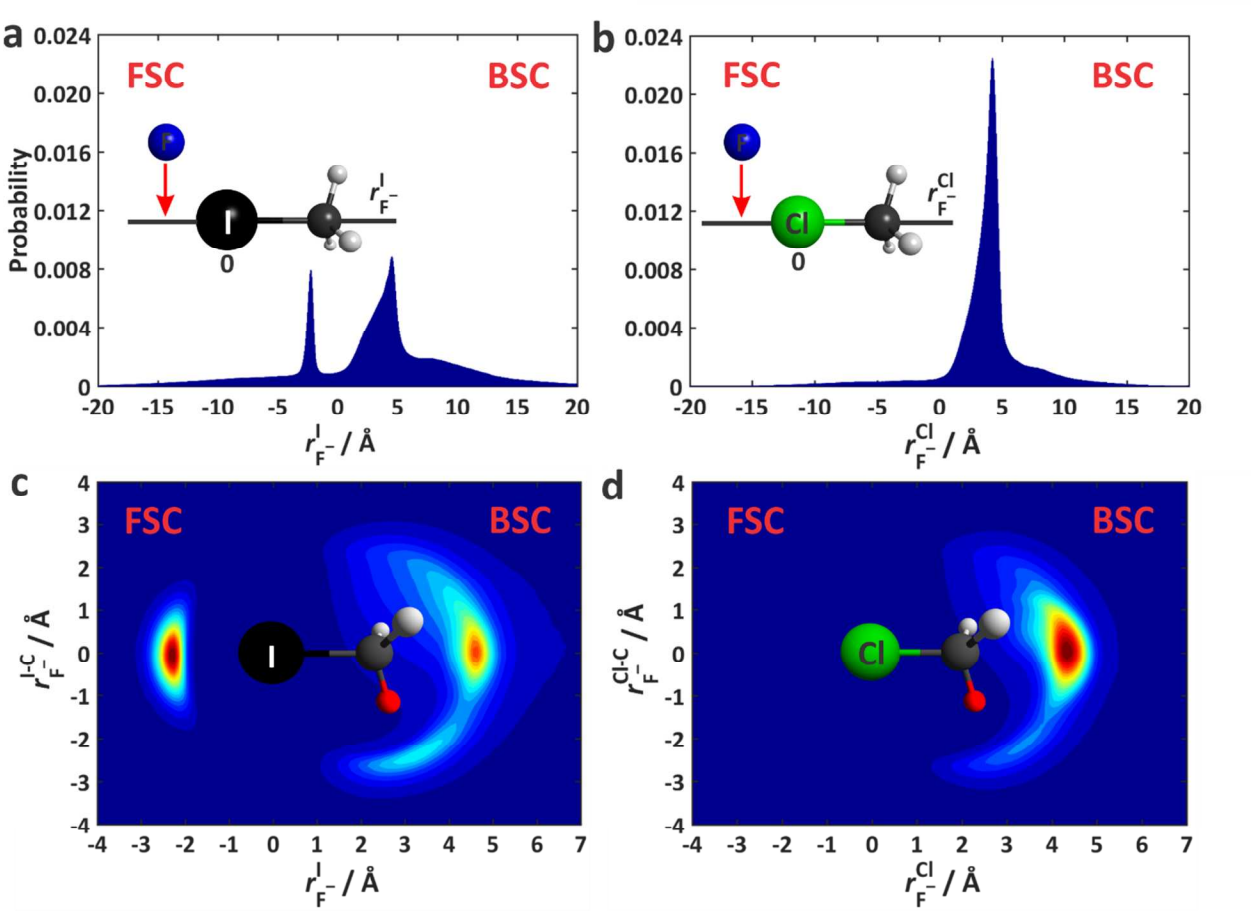

Figure 2. Spatial probabilities of the F^- nucleophile around CH_3Y [Y=Cl,I] on the reactant side of the $F^- + CH_3Y \rightarrow CH_3Y + F^-$ [Y=Cl,I] substitution reactions at the collision energy of 1 kcal mol^{-1} using all the trajectories, which satisfy the following conditions: $r_{C\text{-}Y} < 3.5$ Å and $r_{C\text{-}H} < 2.5$ Å. Normalized distributions were obtained by 1D (a,b) and 2D (c,d) trajectory orthogonal projection (TOP) to the {C,Y} line and to the {Y,C,H(red)} plain as indicated by the structures, respectively, combined with the standard Histogram Analysis method.[21] The front-side and back-side complex regions of the configuration space are denoted with FSC and BSC, respectively. Further spatial probability distributions at collision energies of 4.0, 15.9, 35.3 and 50.0 kcal mol^{-1} are given in the Supporting Information.

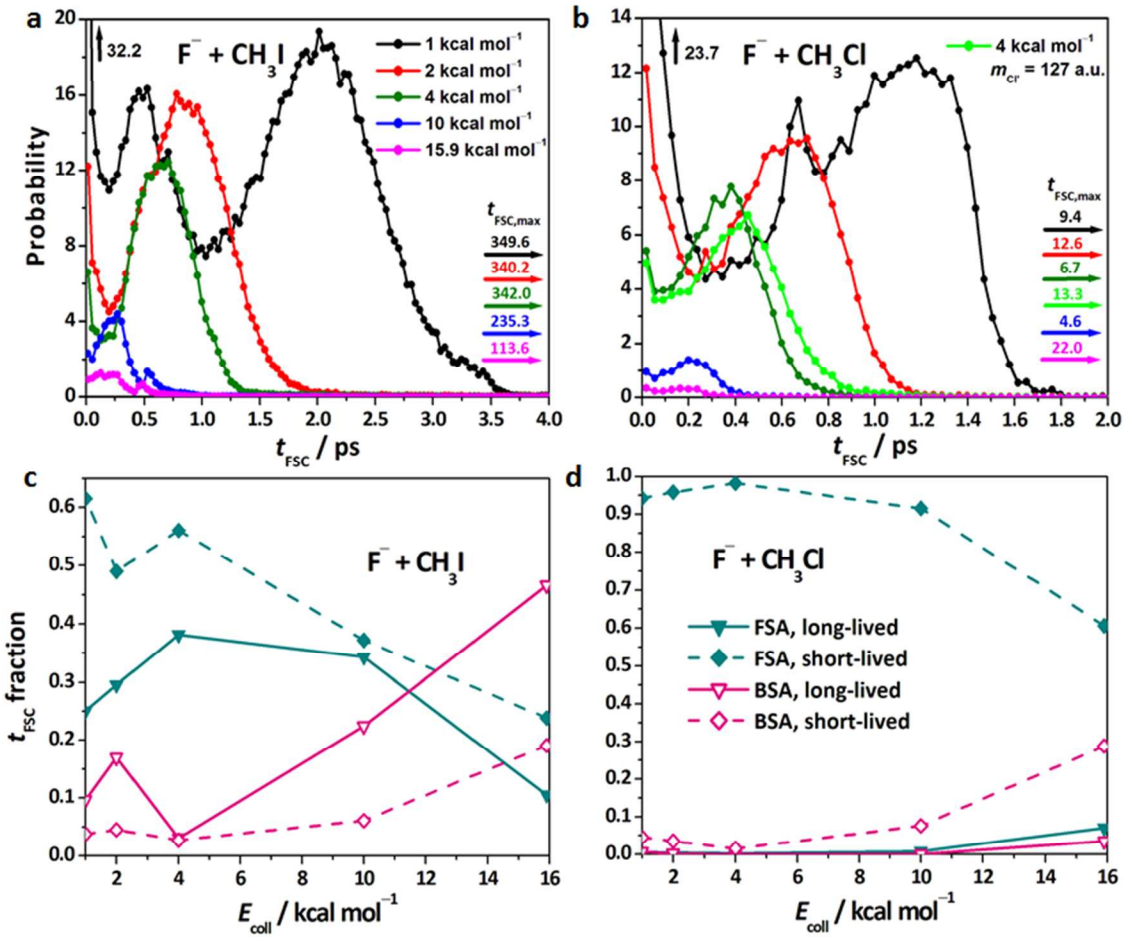

Figure 3. (a,b) Front-side complex life time distributions for the F^- + CH_3Y [Y=Cl,I] S_N2 reactions at different collision energies. The life time is calculated from the trajectory integration time spent by the F^- nucleophile in the front-side region defined as $r_{F^-}^{Y} < 0$, where $r_{F^-}^{Y}$ is the distance of F^- from the Y leaving group after TOP. (c,d) Front-side complex life time fractions split into the individual contribution of trajectories starting with front-side attack (FSA) and back-side attack (BSA). The FSA and BSA trajectories are distinguished based on the initial attack angle defined as the angle between the C-Y vector and the velocity vector of CH_3Y at t = 0. Furthermore, the FSA and BSA are split into the contribution of short-lived (transient) and long-lived (strongly trapped) FSC trajectories. The latter ones are characterized by a life time larger than 2 and 4 ps for Y=Cl and Y=I, respectively.

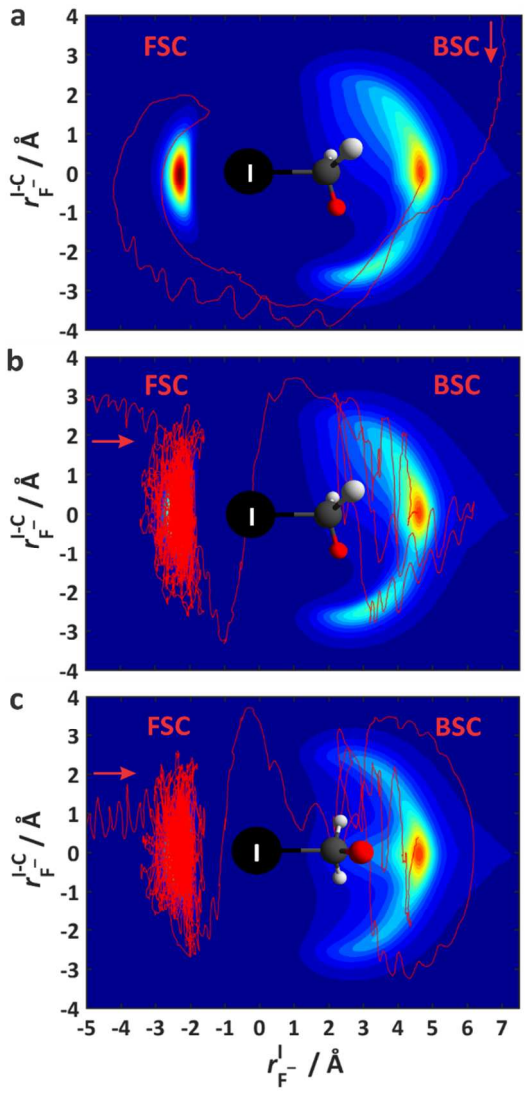

Figure 4. Representative trajectories in the entrance channel of the F^- + CH_3I S_N2 reaction at collision energy of 2 kcal mol^{-1} exhibiting front-side complex (FSC) formation. The dynamics maps were obtained by projection to the planes indicated by the structures on each panel using the 2D TOP method (see text and also Figure 2). (a) Transient short-lived FSC trajectory starting with back-side attack, and showing F^- trapped in the FSC region of the pre-reaction well for 0.6 ps before the reactive S_N2 event. (b,c) Two projections of the same trajectory starting with front-side attack, and featuring long-lived intermediate FSC; the F^- nucleophile is strongly trapped for 42.1 ps before the reactive substitution event.

COMPUTATIONAL METHODS

All the *ab initio* electronic structure computations (geometry optimizations, frequency computations, and potential energy surface scans) were carried out by the Molpro 2015.1 program,[25] except the computation of the molecular orbitals and the Natural Bond Orbital (NBO) population analysis, which were done with the Gaussian 09 program package.[26]

Quasi-classical trajectory (QCT) computations for the F^- + CH_3Y [Y=Cl,I] reactions were performed with our in-house computer code using the recently developed analytical *ab initio* potential energy surfaces.[8,13] The vibrational ground state of the polyatomic reactants CH_3Y [Y=Cl,I] was prepared by normal mode sampling and their rotational temperature was set to 0 K. The initial orientation of CH_3Y [Y=Cl,I] was randomly sampled and the distance between the centers of mass of the reactants was $(x^2+b^2)^{1/2}$, where b is the impact parameter and x was 30/40, 20/30, 20/30, 20/20 and 20/20 bohrs for Y=Cl/I at collision energies of 1, 2, 4, 10 and 15.9 kcal mol^{-1}, respectively. Trajectories were also run at collision energies of 35.3 and 50 kcal mol^{-1} for the F^- + CH_3I reaction with x set to 20 bohrs. b was scanned from 0 to b_{max}, which is the maximum value of b, where any reactive event can occur, with a step size of 0.5 bohr, except at collision energies of 35.3 and 50 kcal mol^{-1}, where a smaller step size of 0.125 bohr was employed in order to get improved statistics for the spatial distributions of the nucleophile. At each b 5000 trajectories were propagated, resulting in more than 2 million trajectories in this study. We also performed dynamics simulations for the mass-scaled reaction F^- + CH_3Cl' by setting the mass of Cl' to 127 a.u. and using the PES of F^- + CH_3Cl.[23] For the exothermic F^- + $CH_3Y \rightarrow CH_3Y + F^-$ [Y=Cl,I] substitution reactions the zero-point energy (ZPE) violation is negligible, thus the QCT product analysis considered all the reactive trajectories. The spatial

distributions of the F^- nucleophile were obtained by the trajectory orthogonal projection (TOP) method combined with the standard Histogram Analysis procedure.

ASSOCIATED CONTENT

Supporting Information

Structures and relative energies of the Nu^---YCH_3 [Nu=F,Cl,Br,I; Y=Cl,Br,I] front-side complexes (Figure S1); Molecular orbitals and atomic charges of the F^---YCH_3 [Y=Cl,I] front-side complexes (Figure S2); Spatial probabilities of the F^- nucleophile around CH_3Y [Y=Cl,I] on the reactant side of the $F^- + CH_3Y \rightarrow CH_3Y + F^-$ [Y=Cl,I] substitution reactions at different collision energies (Figures S3-6); Classical energies of the Nu^---YCH_3 [Nu=F,Cl,Br,I; Y=Cl,Br,I] front-side complex minima (Table S1); Harmonic vibrational frequencies for front-side complex minima (Table S2)

AUTHOR INFORMATION

Corresponding Authors

*E-mail: istvan.szabo@kcl.ac.uk (I.S.), gczako@chem.u-szeged.hu (G.C.).

Notes

The authors declare no competing financial interests.

ACKNOWLEDGMENT

I.S. was supported by the UK EPSRC Fellowship EP/N020669/1. G.C. was supported by the Scientific Research Fund of Hungary (PD-111900) and the János Bolyai Research Scholarship of the Hungarian Academy of Sciences. We acknowledge the National Information Infrastructure

Development Institute for awarding us access to resource based in Hungary at Debrecen and Szeged.

REFERENCES

1. Vollhardt, K. P. C.; Shore, N. E. Organic Chemistry: Structure and Function (W. H. Freeman, **2005**).

2. Hase, W. L. Simulations of Gas-Phase Chemical Reactions: Applications to S_N2 Nucleophilic Substitution. *Science* **1994**, *266*, 998-1002.

3. Chabinyc, M. L.; Craig, S. L.; Regan, C. K.; Brauman, J. I. Gas-Phase Ionic Reactions: Dynamics and Mechanism of Nucleophilic Displacements. *Science* **1998**, *279*, 1882-1886.

4. Mikosch, J.; Trippel, S.; Eichhorn, C.; Otto, R.; Louderaj, U.; Zhang, J.-X.; Hase, W. L.; Weidemüller, M.; Wester, R. Imaging Nucleophilic Substitution Dynamics. *Science* **2008**, *319*, 183-186.

5. Otto, R.; Brox, J.; Trippel, S.; Stei, M.; Best, T.; Wester, R. Single Solvent Molecules Can Affect the Dynamics of Substitution Reactions. *Nature Chem*. **2012**, *4*, 534-538.

6. Xie, J.; Otto, R.; Mikosch, J.; Zhang, J.; Wester, R.; Hase, W. L. Identification of Atomic-Level Mechanisms for Gas-Phase $X^- + CH_3Y$ S_N2 Reactions by Combined Experiments and Simulations. *Acc. Chem. Res.* **2014**, *47*, 2960-2969.

7. Brauman, J. I. Not So Simple. *Science* **2008**, *319*, 168.

8. Szabó, I.; Czakó, G. Revealing a Double-Inversion Mechanism for the $F^- + CH_3Cl$ S_N2 Reaction. *Nat. Commun*. **2015**, *6*, 5972.

9. Stei, M.; Carrascosa, E.; Kainz, M. A.; Kelkar, A. H.; Meyer, J.; Szabó, I.; Czakó, G.; Wester, R. Influence of the Leaving Group on the Dynamics of a Gas-Phase S_N2 Reaction. *Nature Chem.* **2016**, *8*, 151-156.

10. Xie, J.; Hase, W. L. Rethinking the S_N2 Reaction. *Science* **2016**, *352*, 32-33.

11. Liu, P.; Wang, D.; Xu, Y. A New, Double-Inversion Mechanism of the $F^- + CH_3Cl$ S_N2 Reaction in Aqueous Solution. *Phys. Chem. Chem. Phys.* **2016**, *18*, 31895-31903.

12. Szabó, I.; Császár, A. G.; Czakó, G. Dynamics of the $F^- + CH_3Cl \rightarrow FCH_3 + Cl^-$ S_N2 Reaction on a Chemically Accurate Potential Energy Surface. *Chem. Sci.* **2013**, *4*, 4362-4370.

13. Olasz, B.; Szabó, I.; Czakó, G. High-Level Ab Initio Potential Energy Surface and Dynamics of the $F^- + CH_3I$ S_N2 and Proton-Transfer Reactions. *Chem. Sci.* **2017**, *8*, 3164-3170.

14. Cyr, D. M.; Bishea, G. A.; Scarton, M. G.; Johnson, M. A. Observation of Charge-Transfer Excited States in the $I^-•CH_3I$, $I^-•CH_3Br$, and $I^-•CH_2Br_2$ S_N2 Reaction Intermediates Using Photofragmentation and Photoelectron Spectroscopies. *J. Chem. Phys.* **1992**, *97*, 5911-5914.

15. Morris, R. A.; Viggiano, A. A. Kinetics of the Reactions F^- and CF_3Br and CF_3I as a Function of Temperature, Kinetic Energy, Internal Temperature, and Pressure. *J. Phys. Chem.* **1994**, *98*, 3740-3746.

16. Cyr, D. M.; Scarton, M. G.; Wiberg, K. B.; Johnson, M. A.; Nonose, S.; Hirokawa, J.; Tanaka, H.; Kondow, T.; Morris, R. A.; Viggiano, A. A. Observation of the XY^- Abstraction Products in the Ion-Molecule Reactions of $X^- + RY \rightarrow XY^- + R$: An Alternative to the S_N2 Mechanism at Suprathermal Collision Energies. *J. Am. Chem. Soc.* **1995**, *117*, 1828-1832.

17. Xie, J.; Sun, R.; Siebert, M. R.; Otto, R.; Wester, R.; Hase, W. L. Direct Dynamics Simulations of the Product Channels and Atomistic Mechanisms for the $OH^- + CH_3I$ Reaction. Comparison with Experiment. *J. Phys. Chem. A* **2013**, *117*, 7162-7178.

18. Xie, J.; McClellan, M.; Sun, R.; Kohale, S. C.; Govind, N.; Hase, W. L. Direct Dynamics Simulation of Dissociation of the $[CH_3\text{--}I\text{--}OH]^-$ Ion-Molecule Complex. *J. Phys. Chem. A* **2015**, *119*, 817−825.

19. Xie, J.; Otto, R.; Wester, R.; Hase, W. L. Chemical Dynamics Simulations of the Monohydrated $OH^-(H_2O)$ + CH_3I Reaction. Atomic-Level Mechanisms and Comparison with Experiment. *J. Chem. Phys.* **2015**, *142*, 244308.

20. Sun, L.; Song, K.; Hase, W. L. A S_N2 Reaction That Avoids Its Deep Potential Energy Minimum. *Science* **2002**, *296*, 875-878.

21. Szabó, I.; Czakó, G. Mode-Specific Multi-Channel Dynamics of the F^- + CHD_2Cl Reaction on a Global Ab Initio Potential Energy Surface. *J. Chem. Phys.* **2016**, *145*, 134303.

22. Su, T.; Wang, H.; Hase W. L. Trajectory Studies of S_N2 Nucleophilic Substitution. 7. F^- + $CH_3Cl \rightarrow FCH_3 + Cl^-$. *J. Phys. Chem. A* **1998**, *102,* 9819-9828.

23. Sun, L.; Park, K.; Song, K.; Setser, D. W.; Hase, W. L. Use of a Single Trajectory to Study Product Energy Partitioning in Unimolecular Dissociation: Mass Effects for Halogenated Alkanes. *J. Chem. Phys.* **2006**, *124*, 064313.

24. Wang, Y.; Song, H.; Szabó, I.; Czakó, G.; Guo, H.; Yang, M. Mode-Specific S_N2 Reaction Dynamics. *J. Phys. Chem. Lett*. **2016**, *7*, 3322-3327.

25. Werner, H.-J.; Knowles, P. J.; Knizia, G.; Manby, F. R.; Schütz, M.; et al. Molpro, version 2015.1, a package of ab initio programs; see http://www.molpro.net.

26. Frisch, M. J.; et al. Gaussian 09, revision E01; Gaussian, Inc.: Wallingford, CT, **2009**.